The effect of an early planetesimal-driven migration of the giant planets on terrestrial planet formation

K. J. Walsh and A. Morbidelli

University Nice Sophia Antipolis, Laboratoire Cassiopée, Observatoire de la Côte d'Azur, BP 4229, 06304 Nice Cedex 04, France
e-mail: kwalsh@boulder.swri.edu

ABSTRACT

The migration of the giant planets due to the scattering of planetesimals causes powerful resonances to move through the asteroid belt and the terrestrial planet region. Exactly when and how the giant planets migrated is not well known. In this paper we present results of an investigation of the formation of the terrestrial planets during and after the migration of the giant planets. The latter is assumed to have occurred immediately after the dissipation of the nebular disk – i.e. "early" with respect to the timing of the late heavy bombardment (LHB). The presumed cause of our modeled early migration of the giant planets is angular mometum transfer between the planets and scattered planetesimals.

Our model forms the terrestrial planets from a disk of material which stretchs from 0.3–4.0 AU, evenly split in mass between planetesimals and planetary embryos. Jupiter and Saturn are initially at 5.4 and 8.7 AU respectively, on orbits with eccentricities comparable to the current ones, and migrate to 5.2 and 9.4 AU with an e-folding time of 5 Myr.

Unfortunately, the terrestrial planets formed in the simulations are not good analogs for the current solar system, with Mars typically being much too massive. Moreover, the final distribution of the planetesimals remaining in the asteroid belt is inconsistent with the observed distribution of asteroids. This argues that, even if giant planet migration had occurred early, the real evolution of the giant planets would have to have been of the "jumping-Jupiter" type, i.e. the increase in orbital separation between Jupiter and Saturn had to be dominated by encounters between Jupiter and a third, Neptune-mass planet. This result was already demonstrated for late migrations occuring at the LHB time by previous work, and this paper shows those conclusions hold for early migration as well.

Key words. minor planets, asteroids: general – planets and satellites: dynamical evolution and stability – planets and satellites: formation – planets and satellites: general

1. Introduction

The formation of the terrestrial planets is expected to have occurred from a disk of planetesimals in two steps. In the first step, Moon to Mars-size "planetary embryos" formed by runaway and oligarchic accretion (Greenberg et al. 1978; Wetherill & Stewart 1993; Kokubo & Ida 1998). In the second step, the terrestrial planets formed by high-velocity collisions among the planetary embryos (Chambers & Wetherill 1998; Agnor et al. 1999; Chambers 2001; Raymond et al. 2004, 2005, 2006, 2007; O'Brien et al. 2006; Kenyon & Bromley 2006).

The most comprehensive effort to date in modeling terrestrial planet formation (Raymond et al. 2009) focused on 5 constraints of the terrestrial planets: 1. the orbits, particularly the small eccentricities; 2. the masses, with the small mass of Mars the most difficult to match, 3. formation timescales; 4. bulk structure of the asteroid belt and 5. the water content of Earth. Despite success with some of these constraints in each simulation, no simulation satisfied all the constraints simultaneously. For the simulations with fully formed Jupiter and Saturn on nearly circular orbits, the constraint consistently missed is the small mass of Mars. A Mars of the correct size is only obtained in simulations where the giant planets are on orbits with current semimajor axes but much larger eccentricities. This scenario, however, raises the problem of not allowing any water delivery to Earth from material in the outer asteroid belt region. The size of Mars has been a consistent problem for previous works with giant planets assumed on current orbits and disks of planetesimals

and embryos stretching from ~0.5–4.0 AU (Chambers & Wetherill 1998; O'Brien et al. 2006), or even only up to 1.5 or 2.0 AU (Kokubo et al. 2006; Chambers 2001).

However, Hansen (2009) had great success creating analogs of Mars in simulations which begin with a narrow annulus of planetary embryos between 0.7 and 1.0 AU. In these simulations both Mercury and Mars are formed from material that is scattered out of the original annulus by the growing Earth and Venus analogs. In addition, the orbits of the Earth and Venus analogs have eccentricities and inclinations similar to those observed today and the accretion timescales are in agreement, although on the low side, with the ages of the Earth-Moon system deduced from the ^{182}Hf–^{182}W chronometer. This model points to the need for a truncated planetesimal disk at, or near, the beginning of the process of terrestrial planet formation. The origin of this truncation remains to be understood. Similarly, it remains to be clarified how the truncation of the disk of planetesimals at 1 AU can be compatible with the existence of asteroids in the 2–4 AU region.

Nagasawa et al. (2005) and Thommes et al. (2008a) effectively produced a cut in the planetesimal distribution at 1.5 AU by assuming that the giant planets were originally on their current orbits and that secular resonances swept through the asteroid belt during gas-dissipation. However, the assumption that the giant planets orbits had their current semimajor axes when the gas was still present is no longer supported. When embedded in a gas disk, planets migrate relative to each other until a resonance configuration is achieved (Peale & Lee 2002;

Kley et al. 2009; Ferraz-Mello et al. 2003; Masset & Snellgrove 2001; Morbidelli & Crida 2007; Pierens & Nelson 2008). Thus it is believed that the giant planets were in resonance with each other when the gas disk disappeared (Morbidelli et al. 2007; Thommes et al. 2008a; Batygin & Brown 2010) which causes problems in understanding the consequences of the Thommes et al. (2008b) model. Moreover, the Nagasawa et al. (2005) and Thommes et al. (2008a) simulations produce the terrestrial planets too quickly (∼10 Myr), compared to the timing of moon formation indicated by the ^{182}Hf–^{182}W chronometer (>30 Myr and most likely >50 Myr; Kleine et al. 2009) and they completely deplete the asteroid belt by the combination of resonance sweeping and gas-drag (see also Morishima et al. 2010, for a discussion).

The resonant configuration of the planets in a gas disk is extremely different from the orbital configuration observed today. Planetesimal-driven migration is believed to be the mechanism by which the giant planets acquired their current orbits after the gas-disk dissipation. In fact, work by Fernandez & Ip (1984) found that Uranus and Neptune have to migrate outward through the exchange of angular momentum with planetesimals that, largely, they scatter inward. Similarly, Saturn suffers the same fate of outward migration, though Jupiter migrates inward as it ejects the planetesimals from the solar system. The timescale for planetesimal-driven migration of the giant planets depends on the distribution of the planetesimals in the planet-crossing region. It is typically 10 My, with 5 My as the lower bound (Morbidelli et al. 2010). Close encounters between pairs of giant planets might also have contributed in increasing the orbital separations among the giant planets themselves (Thommes et al. 1999; Tsiganis et al. 2005; Morbidelli et al. 2007; Brasser et al. 2009; Batygin & Brown 2010). Beyond the consequences for the scattered planetesimals, the migration of the giant planets affects the evolution of the solar system on a much larger scale, through the sweeping of planetary resonances through the asteroid belt region.

The chronology of giant planet migration is important for the general evolution of the solar system, including the formation of the terrestrial planets. It has been recently proposed (Levison et al. 2001; Gomes et al. 2005; Strom et al. 2005) that the migration of the giant planets is directly linked in time with the so-called "late heavy bombardment" (LHB) of the terrestrial planets (Tera et al. 1974; Ryder 2000, 2002; Kring & Cohen 2002). If this is true, then the migration of the giant planets should have occurred well after the formation of the terrestrial planets. In fact, the radioactive chronometers show that the terrestrial planets were completely formed 100 Myr after the condensation of the oldest solids of the solar system (the so-called calcium alluminum inclusions, which solidified 4.568 Gyr ago; Bouvier et al. 2007; Burkhardt et al. 2008), whereas the LHB occurred 3.9–3.8 Gyr ago. Thus the terrestrial planets should have formed when the giant planets were still on their pre-LHB orbits: resonant and quasi-circular. However, the simulations of Raymond et al. (2009) fail to produce good terrestrial planet analogs when using these pre-LHB orbits.

The alternative possibility is that giant planet-migration occurred as soon as the gas-disk disappeared. In this case, it cannot be a cause of the LHB (and an alternative explanation for the LHB needs to be found; see for instance Chambers 2007). However, in this case giant planet migration would occur while the terrestrial planets are forming, and this could change the outcome of the terrestrial planet formation process. In particular, it is well known that, as Jupiter and Saturn migrate, the strong ν_6 secular resonance sweeps through the asteroid belt down to ∼2 AU (Gomes 1997). The ν_6 resonance occurs when the

precession rate of the longitude of perihelion of the orbit of an asteroid is equal to the mean precession rate of the longitude of perihelion of Saturn, and it affects the asteroids' eccentrcities. If the giant planet migration occurs on a timescale of 5–10 Myr, typical of planetesimal-driven migration, then the ν_6 resonance severely depletes the asteroid belt region (Levison et al. 2001; Morbidelli et al. 2010). This can effectively truncate the disk of planetesimals and planetary embryos, leaving it with an outer edge at about 1.5 AU. Although the location of this edge is not as close to the Sun as assumed in Hansen (2009) (1 AU), it might nevertheless help in forming a Mars analog, i.e. signficantly less massive than the Earth.

An equally important constraint is the resulting orbital distribution of planetesimals in the asteroid belt region, between 2–4 AU. After that region has been depleted of planetesimals and embryos by the sweeping resonances, what remains will survive without major alteration and should compare favorably with todays large asteroids. Studies of late giant planet migration start with an excited asteroid belt, where inclinations already vary from 0–20° (Morbidelli et al. 2010), and cannot match the inclination distribution of the inner asteroid belt with 5 Myr or longer migration timescales. The early migration presented here is different because it occurs immediately after the dissipation of the gas disk so that the planetesimal orbits are dynamically cold, with inclinations less than 1°. Thus, in principle, an early giant planet migration could lead to a different result. Also, the embryos will be present, another difference with late migration scenarios.

The purpose of this paper is to investigate, for the first time, the effect that an *early* migration of the giant planets could have had on the formation of the terrestrial planets and on the final structure of the asteroid belt. In Sect. 2 we discuss our methods and in Sect. 3 we present our results. The conclusions and a discussion on the current state of our understanding of terrestrial planet formation will follow in Sect. 4.

2. Methods

We assume in our simulations that the nebular gas has dissipated, Jupiter and Saturn have fully formed; in the terrestrial planet and asteroid belt region, in the range 0.5–4.0 AU, the planetesimal disk has already formed planetary embryos accounting for half of its total mass. The lifetime of the circumstellar gas disk is observed to be 3–6 Myr, and both Jupiter and Saturn are expected to be fully formed by this time (Haisch et al. 2001). The timescales for oligarchic growth is similar, with lunar to Mars sized embryos growing on million year timescales (Kokubo & Ida 1998, 2000).

The numerical simulations are done using SyMBA, a symplectic *N*-body integrator modified to handle close encounters (Duncan et al. 1998). In our model, the planetary embryos interact with each other; the planetesimals interact with the embryos but not with themselves; all particles interact with the giant planets and, except when specified (explained further below), the giant planets feel the gravity of embryos and planetesimals. Collisions between two bodies result in a merger conserving linear momentum. It has been demonstrated by Kokubo & Genda (2010) that this a priori assumption of simple accretion does not significantly affect the results. The SyMBA code has already been used extensively in terrestrial planet formation simulations (Agnor et al. 1999; Levison & Agnor 2003; O'Brien et al. 2006; McNeil et al. 2005).

2.1. Protoplanetary disk

The initial protoplanetary disks are taken directly from O'Brien et al. (2006), which themselves were based on those of Chambers (2001). The O'Brien et al. (2006) study produced some of the best matches for terrestrial planets and by using similar intial conditions allows a direct comparison. The initial conditions are based on a "minimum mass" solar nebula, with a steep surface density profile. The solid mass is shared between many small planetesimals and a small number of large bodies, the embryos, as suggested by runaway/oligarchic growth simulations (Kokubo & Ida 1998; Kokubo & Ida 2000). In theory, it is possible that, by the time the gas disappears from the disk (which corresponds to time zero in our simulations) the planetary embryos in the terrestrial planet region could have grown larger than the mass of Mars. However, the current mass of Mars seemingly excludes this possibility, and argues for masses to have been martian or sub-martian in mass.

The surface density profile is $\Sigma(r) = \Sigma_0(\frac{r}{1\,\text{AU}})^{-3/2}$, where $\Sigma_0 = 8\,\text{g\,cm}^{-2}$. The distribution of material drops linearly between 0.7 and 0.3 AU. Half of the mass is in the large bodies, of which there were either 25 embryos, each of 0.0933 Earth masses ($M_\oplus$) or 50 embryos of 0.0467 $M_\oplus$. The small bodies are 1/40 as massive as the large embryros, or 1/20 as massive as the small embryos. For all test cases the embryos are spaced between 4–10 mutual hill radii at the beginning of the simulations. In some tests, the smaller planetesimals with an initial semimajor axis larger than 2.0 were cloned into two particles with identical semi-major axis, half the mass in each, and different random eccentricities and inclinations (noted as "Double Asteroids" in Table 1). The initial eccentricities and inclinations were selected randomly in the range of 0–0.01 and 0–0.5 degrees respectively. Thus the initial mass of the disk consisted of 2.6 $M_\oplus$ located inside of 2 AU and a total mass of 4.7 $M_\oplus$.

2.2. Giant planets and migration

In all tests Jupiter and Saturn were started on orbits closer to each other than at the present time, i.e. with semimajor axes of 5.4 and 8.7 AU, respectively. These initial orbits are just beyond their mutual 1:2 mean motion resonance, i.e. the corresponding ratio of orbital periods of Saturn and Jupiter is slightly larger than 2. Even if the giant planets should have started from a resonant configuration – probably the 2:3 resonance (Masset & Snellgrove 2001; Pierens & Nelson 2008) – it is known that secular resonance sweeping through the asteroid belt is important only when the planets' orbital period ratio is larger than 2 (Gomes 1997; Brasser et al. 2009). Thus, our choice of the initial orbits of Jupiter and Saturn is appropriate for the purposes of this study.

Each planet was forced to migrate by imposing a change to their orbital velocities that evolves with time t as:

$$v(t) = v_0 + \Delta v[1 - \exp(-t/\tau)]$$

appropriate Δv to achieve the required change in semimajor axis, and $\tau = 5$ Myr. The latter is the minimum timescale at which planetesimal-driven migration can occur, simply due to the lifetime of planetesimals in the giant planet crossing region, as discussed extensively in Morbidelli et al. (2010). Longer timescales are possible, but previous work has shown that fast timescales affect the asteroid belt region less, and since terrestrial planet formation timescales are in the 10's of millions of years, more rapid migration has a greater chance of affecting the accretion of Mars. Thus, we think that restricting ourselves to the 5 My
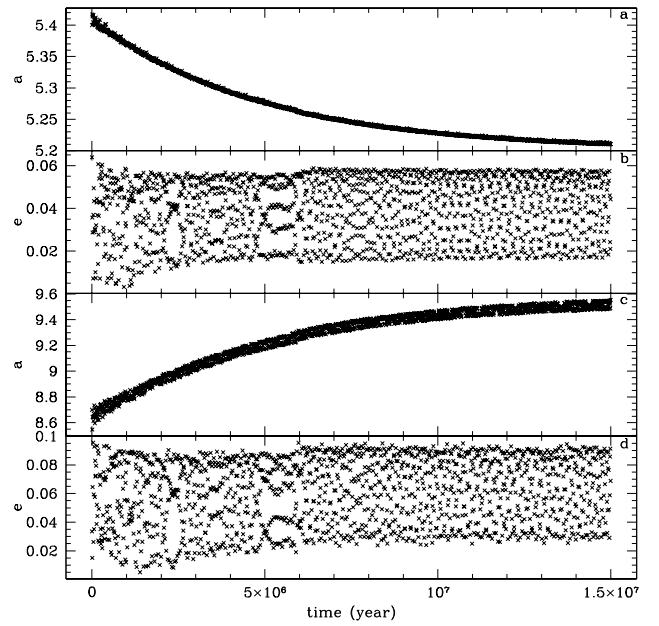

Fig. 1. Example of idealized migration for a system with only Jupiter and Saturn, ending with orbits very close to the current ones. Panel **a)** shows the semimajor axis of Jupiter, **b)** the eccentricity of Jupiter, **c)** the semimajor axis of Saturn and **d)** the eccentricity of Saturn, all plotted as a function of time in years.

timescale is sufficient, as this timescale is the most favorable for these purposes.

If the motion of the giant planets was not affected by the other bodies in the system, the evolution of the eccentricities and inclinations would not change much during migration (Brasser et al. 2009, and Fig. 1). Thus it is relatively simple to find initial conditions that lead to the final orbital configurations with eccentricities and inclinations with mean values and amplitude of oscillations similar to current one. In fact, as shown in Brasser et al. (2009), the initial values $(e_J, e_S) = (0.012, 0.035)$ and $(i_J, i_S) = (0.23°, 1.19°)$, after migration, lead to eccentricities and inclinations whose mean values and amplitudes of oscillation closely resemble those characterizing the current secular dynamics of the giant planets (see Fig. 1).

In our case, however, as the giant planets migrate, they scatter planetesimals and planetary embryos, and their orbits are affected in response. Thus, the final orbits are not exactly like those of Fig. 1. Typically, for instance, the eccentricities and inclinations of the planets are damped, and their relative migration is slightly more pronounced than it was intended to be. Thus, we tried to modify the initial eccentricities of Jupiter and Saturn and the values of Δv in order to achieve final orbits as similar as possible to those of Fig. 1. However, while the effect of planetesimals on the planets is statistically the same from simulation to simulation, (and so can be accounted for by modifying the initial conditions of the planets), the effects of embryos are dominated by single stochastic events. Thus, it is not possible to find planetary initial conditions that lead systematically to good final orbits. In some cases the final orbits are reasonably close to those of the current system, but in many cases they are not. In total we performed 30 simulations. We discarded the simulations with unsuccessful final orbits, and kept only those (9/30) that lead to orbits resembling the current ones. These successful runs are called hereafter "normal migration simulations". Our criterion

Table 1. Simulation results for each simulation.

Run	N	AMD	RMC	M_{planets}	M_{Mars}	a_{Mars}
Normal migration						
Test31	5	0.0085	32.69	2.10	0.56	1.52
Test43	3	0.0011	45.51	1.85	0.59	1.41
Ran1	3	0.0035	58.77	1.82	0.43	1.42
Ran3	4	0.0017	38.95	1.93	0.52	1.52
Ran4	3	0.0023	42.09	1.71	0.14	1.71
Ran7	3	0.0011	50.30	1.76	0.78	1.29
Double asteroids						
Test61	3	0.0023	42.38	1.82	0.59	1.43
Test62	3	0.0014	66.43	1.83	–	–
Double embryos						
Test54	4	0.0011	40.53	1.90	0.06	1.88
Perfect migration						
PM21	4	0.0016	40.87	1.93	0.46	1.41
PM22	3	0.0113	51.34	1.72	0.33	1.37
PM24	6	0.0076	25.93	2.06	0.36	1.43
MVEM	4	0.0014	89.9	1.88	0.11	1.52

Notes. Included are the number of planets N, the angular momentum deficit (AMD) and the radial mass concentration (RMC) for each system of planets, the total mass of the planets M_{planets}, and Mars analog M_{Mars} in Earth Masses, and the semimajor axis of the Mars analogs a_{Mars}. The entry MVEM is data for the current terrestrial planets. Note that Test31 and PM24 each had one embryo stranded in the asteroid belt region, with $a > 2.0$ AU, which are counted in their N, but not used to calculate RMC or AMD.

for discriminating good from bad final orbits was determined after the 15 Myr of migration, and the semimajor axis, eccentricity and oscillation in eccentricity (Δe) were the factors examined. Jupiter's orbit must have had $|a-a_j| < 0.05$, $|e-e_j| < 0.0156$, and $|\Delta e-\Delta e_j| < 0.0164$, while Saturn's orbit required $|a-a_s| < 0.075$, $|e - e_s| < 0.0252$, and $\Delta e - \Delta e_s < 0.0256$.

We complemented our normal migration simulations with what we call hereafter "perfect migration" cases. In these simulations, the planetesimals and embryos do not have any direct effect on the giant planets, even during close encounters. However, their indirect effects cannot be suppressed (specifically the H_{Sun} term from Eq. (32b). in Duncan et al. 1998), but in principle they are weaker. Thus the migration of the giant planets, starting with the initial conditions from Brasser et al. 2009 (as in Fig. 1), met the above criteria in 3 out of 4 simulations. The giant planets had the full gravitational affect on the planetesimals and embryos throughout these simulations, and the mutual effects between planetesimals and embryos remained unchanged.

3. Results

We present the results of 12 simulations of terrestrial planet formation each covering 150 Myr. Of these runs, 9 are normal migration simulations and 3 "perfect migration" simulations (all simulations are listed in Table 1. and refered to by run name, "Test31" etc., throughout). These two sets of simulations had qualitative and quantitative similarities and are thus discussed at the same time and combined in the figures. First, the resulting planets are compared with the current terrestrial planets, followed by a look at the consequences the migration has on the structure of the asteroid belt.
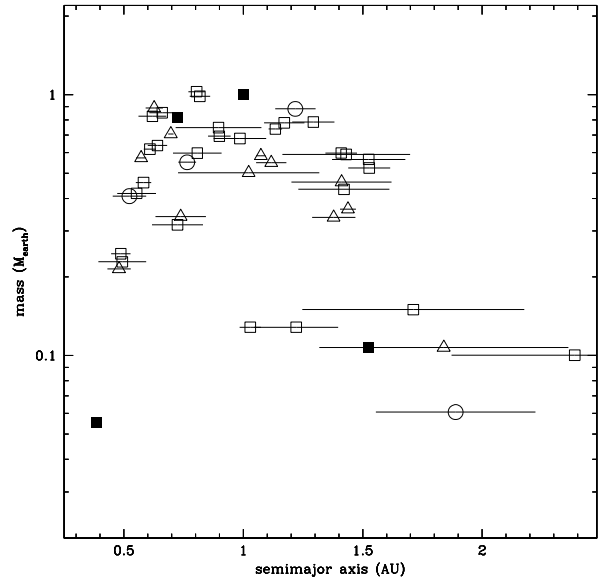
Fig. 2. The final mass ($M_\oplus$) for each planet produced in our simulations is plotted as a function of the planet's semimajor axis. The horizontal error bars show the locations of the perihelion and aphelion of the corresponding orbit. The open squares refer to the planets produced in the normal migration simulations, the open circles to the planets produced in the run with twice as many half-sized embryos, and the open triangles to those produced in the "perfect migration" simulations; the solid squares represent the real terrestrial planets.

3.1. The planets

Results for these simulations are summarized in Fig. 2, where the final masses and semimajor axes of our synthetic planets are compared to those of the real terrestrial planets (see also Table 1). The trend is similar to that found in previous works (see for instance Chambers et al. 2001), where the masses and locations of Earth and Venus are nearly matched by a number of different simulations, but most planets just exterior to Earth, near $a \sim 1.5$ AU are at least 3 times more massive than Mars. However, a handful of planets close to 1.8 AU were of similar mass to Mars. Of note, Test31 had two ~Mars-mass bodies, at 1.2 and 2.4 AU, with an Earth mass planet at 1.52 AU. Test54, the only one of four simulations starting with the smaller embryos with successful migration, produced a sub-Mars mass body at 1.89 AU, just at the edge of the current day asteroid belt. The Ran4 simulation produced a body within 50% of Mars' mass at 1.71 AU, though it had a high eccentricity above 0.13 and was a member of a 3 planet system. In general, planets produced at around 1.5 AU were ~5 times more massive than Mars, and Mars-mass bodies were typically only found beyond 1.7 AU.

The total number of planets produced in each simulation is not systematically consistent with the real terrestrial planet system. Only two simulations produce 4 planets, where we define a "planet" as any embryo-sized or larger body with a semimajor axis less than 2.0 AU. Most simulations had 3 planets at the end, while one produced 5 planets. A common metric for measuring the distribution of mass among multiple planets is the radial mass concentration statistic (RMC), defined as

$$RMC = \max\left(\frac{\sum M_j}{\sum M_j[\log_{10}(a/a_j)]^2}\right), \tag{1}$$

where M_j and a_j are the mass and semimajor axis of planet j (Chambers 2001). The bracketed function is calculated for different a in the region where the terrestrial planets form. The RMC is infinite for a single planet system, and decreases as mass is spread among multiple planets over a range of semimajor axes. The current value of RMC for the solar system is 89.9. For all but one simulation the RMC value is below the current solar systems value, largely due to the large mass concentrated in a Mars-analog orbit (we did not include the two embryos stranded in the asteroid belt region in these calculations, one in Test31 and one in TestPM24). The single simulation with a larger RMC value did not have a Mars analog, and thus the mass was contained in a smaller semimajor axis range.

The terrestrial planets have low eccentricities and inclinations, Earth and Venus both have $e < 0.02$ and $i < 3°$, properties which has proved difficult to match in accretion simulations. O'Brien et al. (2006) and Morishima et al. (2008) reproduced low eccentricities and inclinations largely due to remaining planetesimals which damp the orbital excitation of the planets. A metric used as a diagnostic of the degree of success of the simulations in reproducing the dynamical excitation of the terrestrial planets is the angular momentum deficit (AMD; Laskar 1997):

$$AMD = \frac{\sum_j M_j \sqrt{a_j}\left(1 - \cos(i_j)\sqrt{1 - e_j^2}\right)}{\sum_j M_j \sqrt{a_j}}, \qquad (2)$$

where M_j and a_j are again the mass and semimajor axis and i_j and e_j are the inclination and eccentricity of planet j. The AMD of the current solar system is 0.0014. The AMD for our simulations ranged from 0.0011 to 0.0113. The plantesimal disk used in these simulation is based on that from O'Brien (2006), and is therefore not surprising that some AMDs are consistent with the solar system value. Simulation PM22 is the one with the largest final AMD, because it produced an Earth-analog with a 10° inclination.

Figures 3 and 4 show snapshots of two systems evolving over time. Of interest is the radial clearing caused by the movement of the giant planets and the sweeping of their resonances, particularly the ν_6 resonance. This clearing progresses from the outer edge of the disk towards the Sun, following the migration of the ν_6 resonance, and stops at ~2 AU, which is the final location of this resonance when the giant planets reach their current orbits. Thus, the region of $a > 2.0$ is almost entirely cleared of material in 10 Myr, with only handfuls of planetesimals surviving and a single embryo. At 3 Myr, only $a > 2.5$ AU is largely cleared.

As seen in Fig. 5 the accretion of embryos for the Mars analogs (where a Mars analog is defined as the largest body between 1.2–2.0 AU) begins immediately with ~2 Mars-mass typically being reached in only 2 Myr (note that Fig. 5 shows 12 growth curves, as there are two planets displayed for Test54). Nine of the 11 Mars analogs have reached 0.2 $M_\oplus$ by 3 Myr. At 10 Myr 6 of the 11 have reached 0.3 $M_\oplus$, and by 30 Myr 10 of 11 are above 0.3 $M_\oplus$, or ~3 $M_{\rm Mars}$. One might wonder if our inability to produce a small Mars analog is due to the fact that, in all but one of the presented simulations (Test54 is the exception), the planetary embryos are initially ~one Mars mass. This is not regarded as a problem for the following reasons. First, the Mars analogs with semimajor axes near that of Mars, near 1.5 AU, typically accreted 4 or 5 embryos; thus they consistently accreted much more mass than Mars, and are not simply the result of a chance accretion between two Mars mass embryos. Second, only two of the 11 Mars analogs did not accrete another embryo, in Test54 and Ran4, but both had semimajor axes larger than 1.7 AU, well beyond the current orbit of
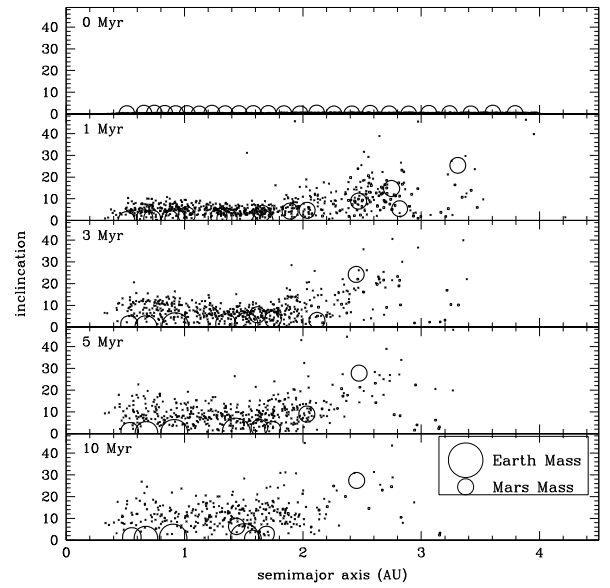

Fig. 3. Evolution of the system over time, showing the clearing of the asteroid belt region with inclination plotted as a function of semimajor axis. The open boxes are planetesimals on orbits within the current asteroid belt region, the crosses are planetesimals elsewhere, and the open circles are embryos or planets scaled in relation to their diameters. The simulation is Test31.
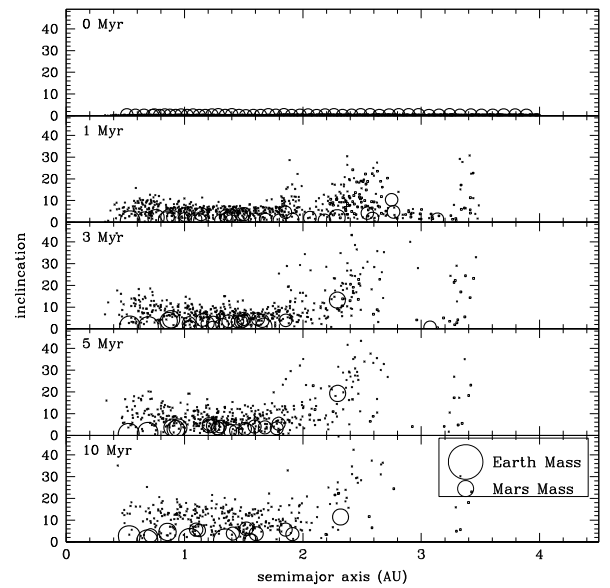

Fig. 4. Same as Fig. 3, but for simulation Test54, which started from 50 embryos of 0.0467 $M_\oplus$ instead of 25 embryos twice as massive.

Mars. Third, our single successful normal migration simulation that started with half-Mars mass embryos also produced an Earth mass planet at 1.2 AU. This planet was already two-Mars masses in 5 Myr (notice that in the same simulation one embryo escaped all collisions with other embryos and therefore remained well below the mass of Mars – see Fig. 5 – but this object ended up at 1.9 AU, well beyond the real position of Mars). Finally, previous works (Chambers 2001; Raymond et al. 2009; Morishima et al. 2010, to quote a few) which started with embryos significantly
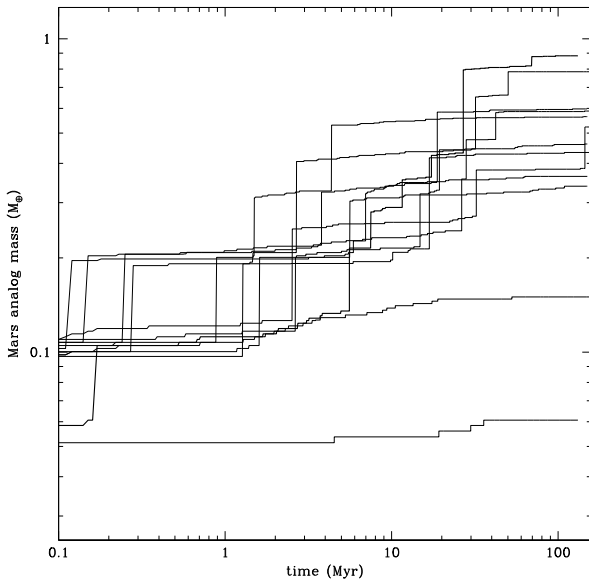
Fig. 5. Mass growth of the Mars analogs for all simulations plotted as a function of time. The most massive Mars analogs exceed the mass of Mars (0.11 $M_\oplus$) in only 2–3 Myr, and then in the next 10–20 Myr continue to grow to their final sizes, ending many times more massive than Mars. The two lines starting from ∼0.05 $M_\oplus$ are for two planets of simulation "Test54", the only successful normal simulation that started with half-Mars mass embryos. The bold line shows the mass growth of the planet ending at ∼1.2 AU; the thin line the planet ending at ∼1.9 AU.

Fig. 6. Endstates of all simulations with the inclination plotted as a function of the semimajor axis with asteroids as open squares, non-asteroid planetesimals as crosses and embryos/planets as open circles scaled by their mass to the 1/3 power.

less massive than Mars met the same Mars-mass problem found here. The similarities between our work and previous in terms of the mass distribution of the synthetic planets as a function of semimajor axis suggest that the giant planet migration does not affect significantly the terrestrial planet accretion process. Thus it is unlikely that small changes in the adopted evolution pattern of the giant planets could lead to significantly different results. Therefore the initial conditions do not appear to be at fault for the failure to match the mass of Mars.

The reason for which the Mars analog consistently grows too massive is twofold. First, they grow fast (in a few million years, as shown in Fig. 5), compared with the timescale required to effectively truncate the disk at ∼2 AU (10 Myr, as shown in Figs. 3 and 4). Second, the truncation of the disk caused by the sweeping of the ν_6 resonance is not sunward enough: the final edge is approximately at 2 AU, whereas an edge at ∼1 AU is needed (Hansen 2009; Kokubo et al. 2006; Chambers 2001).

Figure 6 shows the final incination vs. semimajor axis distributions of all our simulations (respectively, "normal" and "perfect" ones). The sizes of the symbols representing the planets are proportional to the cubic roots of their masses. Again, the problem of the mass of Mars stands out.

3.2. The asteroid belt

In the previous section we have shown that the an early sweeping of secular resonances through the asteroid belt is not useful to solve the small-Mars problem. Here we address the question of other observational constraints. For this purpose, in this section we turn to the asteroid belt, whose orbital distribution is very sensitive to the effects of resonance sweeping (Gomes 1997;
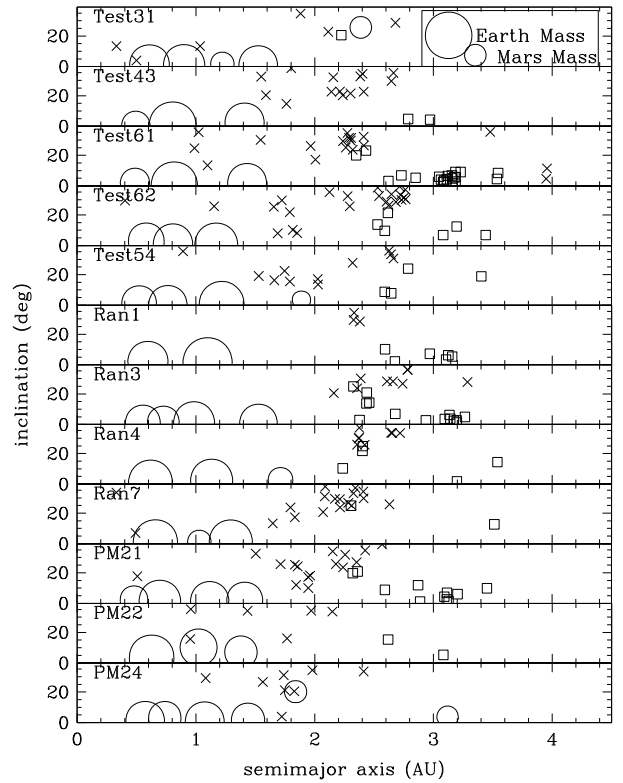
Nagasawa et al. 2000; Minton & Malhotra 2009; Morbidelli et al. 2010).

Morbidelli et al. (2010) have shown that the properties of the asteroid belt after the slow migration of the giant planets are largely incompatible with the current structure of the asteroid belt. However, they assumed that the migration of the giant planets occurred late, after the completion of the process of terrestrial planet accretion and after the primordial depletion/dynamical excitation of the asteroid belt. Thus, that work does not exclude the possibility of an early migration. In fact, the outcome of an early migration could be very different from that of a late migration for two reasons: first, the initial orbits of the plantesimals are quasi-circular and co-planar in the early migration case whereas they are dynamically excited in the late migration case, which is an important difference; second, planetary embryos reside in, or cross, the asteroid belt region during the early time of terrestrial planet formation, and this process has the potential of erasing some of the currently unobserved signatures of resonace sweeping.

To compare the planetesimal distribution obtained in our simulations with the "real" asteroid population, we focus on asteroids larger than ∼50 km in diameter, as in previous works (Petit et al. 2001; Minton & Malhotra 2009; Morbidelli et al. 2010). These bodies are a reliable tracer of the structure of the asteroid belt that resulted from the primordial sculpting process(es), as they are too large to have their orbits altered significantly by the thermal Yarkovsky effect or by collisions (see Fig. 7). Moreover, their orbital distribution (see top panel of
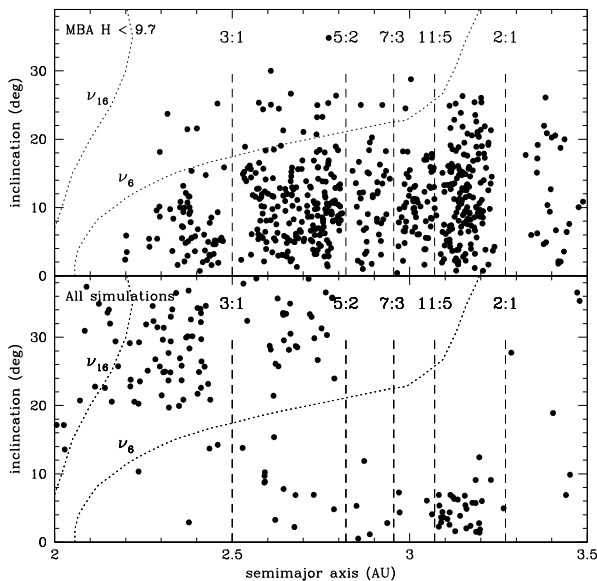
Fig. 7. (*Top*) The inclination of current day asteroids with absolute magnitude $H < 9.7$, corresponding to $D \gtrsim 50$ km, plotted as a function of their semimajor axis. The long-dashed lines show the location of the major mean motion resonances with Jupiter and the short-dashed curves the location of the ν_6 and ν_{16} secular resonances. (*Bottom*) Surviving planetesimals from the 12 simulations, showing a strong depletion of low inclination bodies in the inner part of the asteroid belt region.

Fig. 7) is not affected by observational biases, because all bodies of this size are known (Jedicke et al. 2002).

The final distribution of the planetesimals residing in the asteroid belt in our 12 simulations is shown in the bottom panel of Fig. 7. As can be seen, the difference in orbital distribution between the real belt and that resulting from the giant planet migration process is striking.

A simple metric used in Morbidelli et al. (2010) to quantify the difference in orbital distributions between the real and the synthetic belts is the ratio of asteroids above and below the location of the ν_6 secular resonance with semimajor axis below 2.8 AU. The current day value for asteroids with a diameter above 50 km is 0.07. Combining together all the surviving planetesimals from all our 12 simulations results in a 67/13 ratio, in stark contrast to the current value. Thus, our result is qualitatively similar to that of Morbidelli et al. (2010), even though our resulting ratio is much larger than that obtained in that work (close to 1/1).

The reason for the large ratio obtained in migration simulations, as discussed in Morbidelli et al. (2010), is that the migration of the giant planets forces the ν_6 and ν_{16} secular resonances to move Sun-ward. More precisely, if the orbital separation of Jupiter and Saturn increased by more than 1 AU (as predicted by all models and enacted in our simulations), the ν_6 resonance sweeps the entire asteroid belt as it moves inwards from 4.5 AU to 2 AU; meanwhile the ν_{16} resonance sweeps the belt inside of 2.8 AU to its current location at 1.9 AU (Gomes et al. 1997). In the inner asteroid belt, the ν_{16} resonance sweeps first and the ν_6 resonance sweeps second. The ν_{16} resonance occurs when the precession rate of the longitude of the node of the orbit of an asteroid is equal to the precession rate of the node of the orbit of Jupiter, and it affects the asteroid's orbital inclination. Given the characteristic shape of the ν_6 resonance location in the

(a, i) plane (see Fig. 7), the asteroids that acquire large enough inclination when they are swept by the ν_{16} resonance, avoid being swept by ν_6; thus, their eccentricities are not affected and they remain stable. Conversely, the asteroids that remain at low-to-moderate inclinations after the ν_{16} sweeping are then swept by the ν_6 resonance and their eccentricities become large enough to start crossing the terrestrial planet region. These bodies are ultimately removed by the interaction with the (growing) terrestrial planets. This process favors the survival of high-inclination asteroids (above the current location of the ν_6 resonance) over low-inclination asteroids and explains the large ratio between these two populations obtained in the resonance sweeping simulations. This ratio is larger in our simulations than in those of Morbidelli et al. (2010), because the initial orbits of planetesimals and embryos in our case have small inclinations and eccentricities. Consequently, the secular resonance sweeping can only increase eccentricities and inclinations. Conversely, in the Morbidelli et al. (2010) simulations, the initial orbits covered a wide range of eccentricities and inclinations. Large eccentricities or inclinations can be *decreased* by the secular resonance sweeping. Thus, more objects could remain at low-to-moderate inclinations after the ν_{16} sweeping and fewer objects were removed by the ν_6 sweeping than in our case.

We conclude from our simulations that the migration of the giant planets with an e-folding time of 5 Myr (or longer, as the effects of secular resonance sweeping increases with increasing migration timescale) is inconsistent with the current structure of the asteroid belt, even if it occurred early. In fact, our simulations provide evidence that the planetary embryos crossing the asteroid belt during the process of formation of the terrestrial planets are not able to re-shuffle the asteroid orbital distribution and erase the dramatic scars produced by secular resonance sweeping.

4. Discussion and conclusions

This paper has investigated the effects of *early* giant planet migration on the inner disk of planetesimals and planetary embryos. In the context of solar system formation, "early" is immediately following the disappearance of the gas disk, which is identified as time-zero in our simulations. The giant planets are migrated towards their current orbits with a 5 Myr e-folding time which is appropriate if the migration is caused by planetesimals scattering.

We have shown that the sweeping of secular resonances, driven by giant planet migration, truncates the mass distribution of the inner disk, providing it with an effective outer edge at about 2 AU after about 10 Myr. This edge is too far from the Sun and forms too late to assist in the formation of a small Mars analog. In fact, Chambers (2001) already showed similar results starting from a disk of objects with semi-major axes $0.3 < a < 2.0$ AU, the terrestrial planet accretion process leads to the formation of planets that are systematically 3–5 times too massive at ~1.5 AU. For completeness, we have continued our simulations well beyond the migration timescale of the giant planets to follow the accretion of planets in the inner solar system, and we have confirmed Chambers (2001) result.

Hansen (2009) showed that obtaining planets at ~1.5 AU that have systematically one Mars mass requires that the disk of solid material in the inner solar system had an outer edge at about 1 AU. The inability of secular resonance sweeping during giant planets migration to create such an edge suggests that a different mechanism needs to be found.

Moreover, our study adds to the continuing inability of models with a slow migration of the giant planets, $\tau \gtrsim 5$ Myr, to leave an asteroid belt with a reasonable inclination distribution. Morbidelli et al. (2010) argued that the only possibility for the orbits of Jupiter and Saturn to move away from each other on a timescale shorter than 1 Myr is that an ice giant planet (presumably Uranus or Neptune) is first scattered inwards by Saturn and is subsequently scattered outwards by Jupiter, so that the two giant planets recoil in opposite directions. They dubbed this a "jumping-Jupiter" evolution and showed that in this case the final orbital distribution of the asteroid belt is consistent with that observed. Again, Morbidelli et al. (2010) worked in the framework of a "late" displacement of the orbits of the giant planets. Our results in this paper suggest that a jumping-Jupiter evolution would also be needed in the framework of an "early" displacement of the orbits of the giant planets.

At this point, it is interesting to speculate what the effects of an "early" jumping-Jupiter evolution would be on the terrestrial planet formation process. In essence, an early jumping-Jupiter evolution would bring the giant planets to current orbits at a very early time. So, the outcome of the terrestrial planet formation process would resemble that of the simulations of Raymond et al. (2009) with giant planets initially with their current orbital configuration, labelled "EJS" in that work. In these simulations, though, (see their Fig. 10), the Mars analog is, again, systematically too big. It is questionable whether a jumping-Jupiter evolution could bring the giant planets onto orbits with current semimajor axes but larger eccentricities, as required in the most successful simulations of Raymond et al. (2009), labelled "EEJS". However, even though jumping-Jupiter evolutions satisfying this requirement were found, it is important to note that all of the outcomes of the EEJS simulations of Raymond et al. (2009). While producing a small Mars in several cases, the EEJS simulations failed in general to bring enough water to the terrestrial planets, formed the Earth too early compared to the nominal timescale of 50 Myr and left the terrestrial planets on orbits too dynamically excited. For all these reasons an early jumping-Jupiter evolution is not a promising venue to pursue for a successful model of terrestrial planet formation.

In conclusion, our work substantiates the problem of the small mass of Mars and suggests that understanding terrestrial planet formation requires a paradigm shift in our view of the early evolution of the solar system.

References

Agnor, C., Canup, R., & Levison, H. 1999, Icarus, 142, 219
Batygin, K., & Brown, M. E. 2010, ApJ, 716, 1323
Bouvier, A., Blichert-Toft, J., Moynier, F., Vervoort, J. D., & Albarède, F. 2007, Geochim. Cosmochim. Acta, 71, 1583
Burkhardt, C., Kleine, T., Bourdon, B., et al. 2008, Geochim. Cosmochim. Acta, 72, 6177
Brasser, R., Morbidelli, A., Gomes, R., Tsiganis, K., & Levison, H. F. 2009, A&A, 507, 1053
Chambers, J. 2001, Icarus 152, 205
Chambers, J. 2007, Icarus 189, 386
Chambers, J. E., & Wetherill, G. W. 1998, Icarus, 136, 304
Duncan, M. J., Levison, H. F., & Lee, M. H. 1998, ApJ, 116, 2067
Fernandez, J. A., & Ip, W. 1984, Icarus, 58, 109
Ferraz-Mello, S., Beaug, C., & Michtchenko, T. A. 2003, CeMDA, 87, 99
Gomes, R., Levison, H., Tsiganis, K., & Morbidelli, A. 2005, Nature, 435, 466
Gomes, R. S. 1997, AJ, 114, 396
Greenberg, R., Hartmann, W. K., Chapman, C. R., & Wacker, J. F. 1978, Icarus, 35, 1
Hansen, B. M. S. 2009, ApJ, 703, 1131
Jedicke, R., Larsen, J., & Spahr, T. 2002, in Asteroids III ed. W. F. Bottke, A. Cellino, P. Paolicchi, & R. P. Binzel (Tucson, Arizona: Univ. Arizona Press)
Kenyon, S. J., & Bromley, B. C. 2006, AJ, 131, 1837
Kleine, T., Touboul, M., & Bourdon, B. 2009, Geochim. Cosmochim. Acta, 73, 5150
Kley, W., Bitsch, B., & Klahr, H. 2009, A&A, 506, 971
Kokubo, E., & Genda, H. 2010, ApJ, 714, L21
Kokubo, E., & Ida, S. 1998, Icarus, 131, 171
Kokubo, E., & Ida, S. 2000, Icarus, 143, 15
Kokubo, E., Kominami, J., & Ida, S. 2006, ApJ, 642, 1131
Kring, D. A., & Cohen, B. A. 2002, JGRE, 107, 5009
Laskar, J. 1997, A&A, 317, L75
Levison, H. F., Dones, L., Chapman, C. R., et al. 2001, Icarus, 151, 286
Levison, H. F., & Agnor, C. 2003, ApJ, 125, 2692
Masset, F., & Snellgrove, M. 2001, MNRAS, 320, 55
McNeil, D., Duncan, M., & Levison, H. F. 2005, ApJ, 130, 2884
Minton, D. A., & Malhotra, R. 2009, Nature, 457, 1109
Morbidelli, A., & Crida, A. 2007, Icarus, 191, 158
Morbidelli, A., Brasser, R., Gomes, R., Levison, H. F., & Tsiganis, K. 2010, AJ, 140, 1391
Morishima, R., Schmidt, M. W., Stadel, J., & Moore, B. 2008, ApJ, 685, 1247
Morishima, R., Stadel, J., & Moore, B. 2010, Icarus, 207, 517
Nagasawa, M., & Lin, D. N. C. 2005, ApJ, 632, 1140
Nagasawa, M., Tanaka, H., & Ida, S. 2000, AJ, 119, 1480
O'Brien, P., Morbidelli, A., & Levison, H. 2006, Icarus, 184, 39
Peale, S. J., & Lee, M. H. 2002, Science, 298, 593
Petit, J.-M., Morbidelli, A., & Chambers, J. 2001, Icarus, 153, 338
Pierens, A., & Nelson, R. 2008, A&A, 482, 333
Raymond, S. N., Quinn, T., & Lunine, J. I. 2004, Icarus, 168, 1
Raymond, S. N., Quinn, T., & Lunine, J. I. 2005, ApJ, 632, 670
Raymond, S. N., Quinn, T., & Lunine, J. I. 2006, Icarus, 183, 265
Raymond, S. N., Quinn, T., & Lunine, J. I. 2007, Astrobiology, 7, 66
Raymond, S. N., O'Brien, D. P., Morbidelli, A., & Kaib, N. A. 2009, Icarus, 203, 644
Ryder, G. 2002, J. Geophys. Res. Planets, 107, 5022
Ryder, G., Koeberl, C., & Mojzsis, S. 2000, in Origin of the Earth and Moon, ed. R. Canup, & R. Knighter (Tucson, Arizona: Univ. Arizona Press)
Strom, R. G., Malhotra, R., Ito, T., Fumi, Y., & Kring, D. A. 2005, Science, 309, 1847
Tera, F., Papanastassiou, D. A., & Wasserburg, G. J. 1974, E&PSL, 22, 1
Thommes, E. W., Duncan, M. J., & Levison, H. F. 1999, Nature, 402, 635
Thommes, E., Nagasawa, M., & Lin, D. N. C. 2008a, ApJ, 676, 728
Thommes, E. W., Bryden, G., Wu, Y., & Rasio, F. A. 2008b, ApJ, 675, 1538
Tsiganis, K., Gomes, R., Morbidelli, A., & Levison, H. 2005, Nature, 435, 459
Wetherill, G. W., & Stewart, G. R. 1993, Icarus, 106, 190